VAPOR FLOW IN THE CONDENSER OF A GAS-REGULATED HEAT PIPE

A. A. Parfent'eva and V. D. Portnov

UDC 536.58

Vapor flow in the condenser of a cylindrical gas-regulated heat pipe is considered in a broad range of Reynolds numbers with uniform suction at the wall.

At present, in calculating gas-regulated heat pipes (GRHP), the boundary of the vapor–gas front (VGF) is often regarded as plane. On the basis of experimental data and visual observations, it was shown in [1, 2] that this is not always so. Often the front is parabolic. In connection with this, there arises the question of mathematical description of the flow in GRHP and, in particular, in the VGF region.

The hydrodynamics of vapor flow in ordinary non-gas-regulated heat pipes has been investigated in numerous works [3-9]. In GRHP, the presence of uncondensed gas leads to the existence of a zone of hydrodynamic interaction between the vapor and the gas, which influences the velocity field and the pressure distribution over the heat pipe.

The present investigation is prompted by the lack of consistent theoretical and experimental data on the hydrodynamics of vapor flow in a GRHP condenser, especially in the VGF region. This problem is divided into two stages: 1) determining the velocity profile and hydrodynamics of the vapor flow in the active region of the condenser; 2) finding the VGF dimensions by using the velocity profiles obtained in the first stage of solving the problem.

The flow in the active region of the condenser is described using the equations of motion in cylindrical coordinates:

$$\tilde{U}\frac{\partial\tilde{U}}{\partial\tilde{X}}+\tilde{V}\frac{\partial\tilde{U}}{\partial\tilde{Y}}=-\frac{1}{\rho}\frac{\partial\tilde{P}}{\partial\tilde{X}}+\nu\left[\frac{1}{\tilde{Y}}\frac{\partial}{\partial\tilde{Y}}\left(\tilde{Y}\frac{\partial\tilde{U}}{\partial\tilde{Y}}\right)+\frac{\partial^2\tilde{U}}{\partial\tilde{X}^2}\right] \tag{1}$$

$$\tilde{U}\frac{\partial\tilde{V}}{\partial\tilde{X}}+\tilde{V}\frac{\partial\tilde{V}}{\partial\tilde{Y}}=-\frac{1}{\rho}\frac{\partial\tilde{P}}{\partial\tilde{Y}}+\nu\left[\frac{1}{\tilde{Y}}\frac{\partial}{\partial\tilde{Y}}\left(\tilde{Y}\frac{\partial\tilde{V}}{\partial\tilde{Y}}\right)-\frac{\tilde{V}}{\tilde{Y}^2}+\frac{\partial^2\tilde{V}}{\partial X^2}\right] \tag{2}$$

and the mass conservation equation:

$$\frac{\partial(\tilde{Y}\tilde{U})}{\partial\tilde{X}}+\frac{\partial(\tilde{Y}\tilde{V})}{\partial\tilde{Y}}=0. \tag{3}$$

Eliminating the pressure from Eqs. (1) and (2) and switching to dimensionless variables

$$\tilde{U}=V_0U,\ \tilde{V}=V_0VR/L;\quad \tilde{X}=LX;\quad \tilde{Y}=RY;\quad B=L/R;\quad \mathrm{Re}_r=\frac{V_0R}{\nu}, \tag{4}$$

it is found that

$$\frac{\partial U}{\partial X}\frac{\partial U}{\partial Y}+U\frac{\partial^2U}{\partial X\partial Y}+\frac{\partial V}{\partial Y}\frac{\partial U}{\partial Y}+V\frac{\partial^2U}{\partial Y^2}-\frac{1}{B^2}\frac{\partial U}{\partial X}\frac{\partial V}{\partial X}-$$

$$-\frac{1}{B^2}U\frac{\partial^2V}{\partial X^2}-\frac{1}{B^2}\frac{\partial V}{\partial X}\frac{\partial V}{\partial Y}-\frac{1}{B^2}V\frac{\partial^2V}{\partial X\partial Y}=\frac{B}{\mathrm{Re}_r}\frac{\partial}{\partial Y}\left[\frac{1}{Y}\frac{\partial}{\partial Y}\left(Y\frac{\partial U}{\partial Y}\right)\right]+$$

$$+\frac{1}{B\,\mathrm{Re}_r}\frac{\partial^3U}{\partial X^2\partial Y}-\frac{1}{B\,\mathrm{Re}_r}\frac{\partial}{\partial X}\left[\frac{1}{Y}\frac{\partial}{\partial Y}\left(Y\frac{\partial V}{\partial Y}\right)\right]+\frac{1}{B\,\mathrm{Re}_rY^2}\frac{\partial V}{\partial X}-\frac{1}{B^3\,\mathrm{Re}_r}\frac{\partial^3V}{\partial X^3}, \tag{5}$$

Moscow Power Institute. Translated from Inzhenerno-Fizicheskii Zhurnal, Vol. 47, No. 3, pp. 427-432, September, 1984. Original article submitted May 13, 1983.

0022-0841/84/4703-1061$08.50

$$\frac{\partial (YU)}{\partial X} + \frac{\partial (YV)}{\partial Y} = 0. \tag{6}$$

The current function ψ is now introduced:

$$U = \frac{1}{Y}\frac{\partial \psi}{\partial Y}; \quad V = -\frac{1}{Y}\frac{\partial \psi}{\partial X}. \tag{7}$$

The solution of Eq. (5) is sought in polynomial form:

$$\psi = 2B(1-X)Y^2\left(1-\frac{Y^2}{2}\right) + (1-Y^2)^2\sum_{i=0}^{2} A_{2i+1}X^{2i+1}Y^{6i+2}, \tag{8}$$

satisfying the boundary conditions

$$\begin{gathered} 1)\ \psi = B \text{ when } X=0;\ Y=1;\ 2)\ \psi=0 \text{ when } X=1;\ Y=1;\ 3)\ V=0 \text{ when } Y=0; \\ 4)\ U=0 \text{ when } Y=1;\ 5)\ V=B \text{ when } Y=1;\ 6)\ \frac{\partial U}{\partial Y}=0 \text{ when } Y=0. \end{gathered} \tag{9}$$

Taking account of Eq. (7), the following expressions are obtained for the axial and radial components of the velocity:

$$U = 4B(1-X)(1-Y^2) + 2A_1X(1-4Y^2+3Y^4) + 4A_3X^3Y^6(2-5Y^2+3Y^4), \tag{10}$$

$$V = 2BY\left(1-\frac{Y^2}{2}\right) - A_1Y(1-Y^2)^2 - 3A_3X^2Y^7(1-Y^2)^2. \tag{11}$$

In Eqs. (10) and (11), the coefficients A_1 and A_3 are unknown. They are found by transforming differential equation (5) taking account of Eqs. (9)-(11) for ψ, U, and V. As a result, an ordinary algebraic equation is obtained:

$$F = 3B^2(1-X)f_1 + 8A_1B(1-X)f_2 + 24A_3BX^2f_3 + 4A_1BXf_4 + 8A_1^2Xf_5 + 8A_1A_3X^3f_6 + 2A_3BX^3f_7 + 16A_3^2X^5f_8 +$$

$$+ 3\frac{A_3}{B}Xf_9 - 6\frac{A_1A_3}{B^2}Xf_{10} + 6\frac{A_3}{B}(1-X)f_{11} + 3\frac{A_3^2}{B^2}X^3f_{12} - 24\frac{A_3}{B\,\mathrm{Re}_r}Xf_{13} - 48\frac{A_1B}{\mathrm{Re}_r}Xf_{14} - 96A_3\frac{B}{\mathrm{Re}_r}f_{15} = 0, \tag{12}$$

where

$$\begin{gathered} f_1 = Y - Y^3;\ f_2 = -2Y + 5Y^3 - 3Y^5;\ f_3 = 6Y^5 - 26Y^7 + 35Y^9 - 15Y^{11}; \\ f_4 = Y + 2Y^3;\ f_5 = -Y + 4Y^3 - 6Y^5 + 3Y^7;\ f_6 = 3Y^5 - 48Y^7 + 85Y^9 - 102Y^{11} + \\ + 42Y^{13};\ f_7 = 45Y^5 - 256Y^7 + 340Y^9 - 108Y^{11};\ f_8 = 12Y^{11} - 56Y^{13} + 104Y^{15} - \\ - 90Y^{17} + 30Y^{19};\ f_9 = 6Y^7 - 19Y^9 + 18Y^{11} - 5Y^{13};\ f_{10} = Y^7 - 4Y^9 + 6Y^{11} - \\ - 10Y^{13} + Y^{15};\ f_{11} = Y^7 - 3Y^9 + 3Y^{11} - 2Y^{13};\ f_{12} = -5Y^{13} + 24Y^{15} - 42Y^{17} + \\ + 32Y^{19} - 9Y^{21};\ f_{13} = 6Y^5 - 20Y^7 + 15Y^9;\ f_{14} = Y;\ f_{15} = 3Y^3 - 20Y^5 + 25Y^7. \end{gathered}$$

Using the Galerkin method [10], the unknown coefficients A_1 and A_3 are found from the system of equations

$$\int_0^1\int_0^1 F\varphi_1 dXdY = 0, \quad \int_0^1\int_0^1 F\varphi_2 dXdY = 0, \tag{13}$$

where $\varphi_1 = XY^2(1-Y^2)^2$ and $\varphi_2 = X^3Y^8(1-Y^2)^2$ are functions with the coefficients A_1 and A_3 in Eq. (8).

Solving Eq. (13) with fixed values of the geometric parameter B and the radial Reynolds number (Re_r), the coefficients A_1 and A_3 are obtained; knowing these, the profiles of the velocities U and V may be obtained from Eqs. (10) and (11).

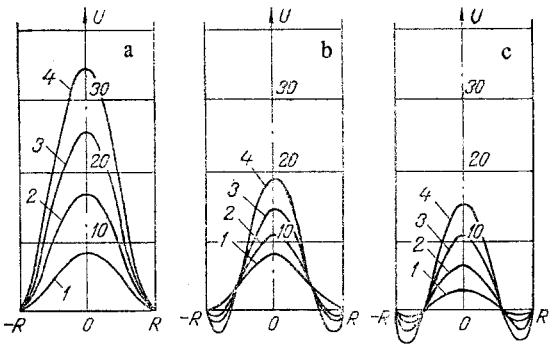

Fig. 1. Theoretical axial-velocity profiles with Re_r = 1 (1), 2 (2), 3 (3), and 4 (4) in different cross sections of the condenser: a) X = X_*; b) X = = 0.95; c) X = 1.0.

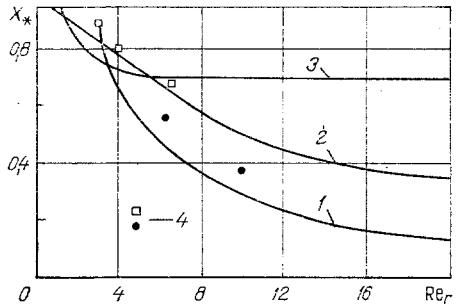

Fig. 2. Coordinates of onset of return flow with different Re_r: 1) calculation of [9]; 2) present calculation; 3) calculation of [11]; 4) experimental data of [9].

In the first approximation, the velocity profiles and pressure differences in the active region of the condenser are calculated with an accuracy allowing for the one unknown coefficient A_1, which is calculated from the equation

$$0.1142\,A_1^2 - \left(0.267 - \frac{2.69}{\mathrm{Re}_r}\right) BA_1 - 0.133B^2 = 0, \tag{14}$$

obtained from the first relation in Eq. (13) with $A_3 = 0$.

The axial-velocity profiles with Re_r = 1-4 in different condenser cross sections are shown in Fig. 1. As is evident from Fig. 1, there is return flow at the end of the active region of the condenser. The extent of the return-flow region here increases as the Reynolds number increases. For example, when $Re_r = 1$, the coordinate of onset of return flow $X_* = 0.948$, and when $Re_r = 4$, $X_* = 0.77$. This is clearly evident in Fig. 2. In the first approximation ($A_3 = 0$), the coordinates X_* are found from the condition that the tangential stress at the wall vanishes, i.e., $\partial U/\partial Y = 0$, and differentiation of Eq. (10) at the wall (Y = 1) leads to the expression $X_* = B/[B + A_1(B, Re_r)]$. The results of this calculation are in good agreement with the experimental results of [9].

Knowing the velocity profiles in the return-flow region in the GRHP, the VGF dimensions ΔX may be approximately determined (Fig. 3). These dimensions are determined by extrapolating points of inflection of the velocity in the VGF region. As is evident from Fig. 3, ΔX is larger at large Re_r. The VGR region is approximated by an ordinary quadratic parabola in the solution.

The component of the pressure gradient along the heat pipe is determined from Eq. (1). After transformation, it is found that

$$\frac{\partial P}{\partial X} = \frac{B}{\mathrm{Re}_r}\left[\frac{1}{Y}\frac{\partial}{\partial Y}\left(Y\frac{\partial U}{\partial Y}\right)\right] - U\frac{\partial U}{\partial X} - V\frac{\partial U}{\partial Y}. \tag{15}$$

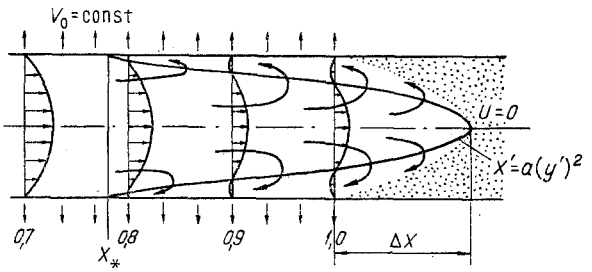

Fig. 3. Return-flow region and vapor–gas front at $Re_r = 4$; $X_* = 0.768$; $\Delta X \approx 0.19$.

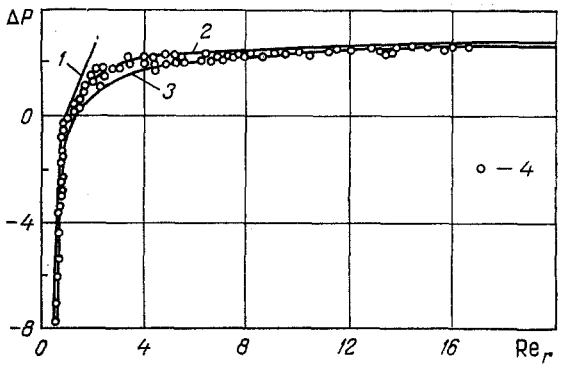

Fig. 4. Variation in dimensionless pressure on the active region of the heat-pipe condensation zone: 1) calculation on the basis of velocity similarity over the length of the pipe; 2) present solution; 3) calculation of [9]; 4) experimental data of [9].

Integrating Eq. (15) over the whole active region of the condenser gives a relation for the variation in axial pressure at the axis (Y = 0):

$$\Delta P_x = 7.2B^2\left(1-\frac{1}{\mathrm{Re}_r}\right)-14.4\,\frac{A_1B}{\mathrm{Re}_r}-1.8A_1^2; \tag{16}$$

at the wall (Y = 1):

$$\Delta P_x = 3.6B^2\left(1-\frac{2}{\mathrm{Re}_r}\right)-3.6\,A_1B\left(1+\frac{4}{\mathrm{Re}_r}\right)-A_3B\left(1.6-\frac{42.3}{\mathrm{Re}_r}\right). \tag{17}$$

The pressure differences in the active region of the GRHP condenser may be calculated from these relations. The results of calculating the variation in dimensionless pressure on the section from $X_1 = 0.05$ to $X_2 = 0.95$ are shown in Fig. 4. As is evident from Fig. 4, the results are in good agreement with the experimental data of [9].

The theoretical relations proposed here allow the velocity profiles, pressure differences, and coordinates of onset of reverse flow to be sufficiently accurately determined over the whole active region of the condenser when $Re_r \leq 20$ and allow the dimensions of the vapor–gas front to be estimated with different geometric dimensions and power inputs to the GRHP.

Note also that in real GRHP, under the action of the return flows, smearing of the VGF will occur on account of the friction between vapor and gas, i.e., the problem is conjugate. Mathematical description of this problem entails considerable difficulties. Experimental investigations are necessary to refine the VCF dimensions. Analysis of theoretical and experimental results offers the possibility of taking account of the nonlinearity and extent of the VGF in GRHP calculations and construction.

NOTATION

$\tilde{U}$, axial velocity component; U, dimensionless axial velocity component; V_0, suction rate at wall; $\tilde{V}$, radial velocity component; $\tilde{P}$, static pressure; P, dimensionless pressure; R, heat

pipe radius; L, length of active region of condenser; Re_r, radial Reynolds number; $\tilde{X}$, axial coordinate; $\tilde{Y}$, radial coordinate; Y, dimensionless radial coordinate; B, geometric parameter; ρ, density; ν, kinematic viscosity; ψ, current function; V, dimensionless radial velocity component; X, dimensionaless axial coordinate.

LITERATURE CITED

1. A. A. Parfent'eva, V. D. Portnov, V. Ya. Sasin, and Yu. N. Domnitskii, "Visual investigations of the vapor–gas front in a gas-regulated heat pipe," Tr. Mosk. Energ. Inst., No. 448, 44-50 (1980).
2. V. V. Galaktionov, A. A. Parfent'eva, V. D. Portnov, and V. Ya. Sasin, "Boundary of a vapor–gas front in the condenser of a plane gas-regulated heat pipe," Inzh.-Fiz. Zh., 42, No. 3, 387-392 (1982).
3. T. P. Cotter, "Theory of heat pipe," LA-3246-M (1965), pp. 11-41.
4. A. S. Berman, "Laminar flow in channels with porous walls," J. Appl. Phys., 24, No. 9, 1232-1235 (1953).
5. S. W. Juan and A. B. Finkelstein, "Laminar flow with injection and suction through porous wall," Trans. ASME, 75, 719-724 (1956).
6. R. M. Terrill and P. W. Thomas, "On laminar flow through a uniformly porous pipe," Appl. Sci. Res., 21, 37-67 (August, 1969).
7. C. A. Bankston and H. I. Smith, "Incompressible laminar flow in cylindrical heat pipes," ASME Paper 71-WA/HT-IS (1971), pp. 1-10.
8. C. A. Bakston and H. I. Smith, "Vapor flow in cylindrical heat pipes," J. Heat Trans., 371-376 (August, 1973).
9. Kveil and Levi, "Laminar flow in a tube with suction through a porous wall," Teploperedacha, No. 1, 66-72 (1975).
10. L. V. Kantorovich and V. I. Krylov, Approximate Methods of Higher Analysis [in Russian], Gos. Izd. Tekh.-Teor. Lit., Moscow–Leningrad (1952), pp. 290-301.
11. P. I. Bystrov and V. S. Mikhailov, "Laminar flow of a vapor current in the condensation region of heat pipes," Teplofiz. Vys. Temp., 20, No. 2, 311-316 (1982).

THEORY OF AN ABSOLUTE SUPERCONDUCTING BOLOMETRIC THERMAL-RADIATION RECEIVER

S. B. Kiselev

UDC 535.6:621.317.794

Taking the transient zone into account, a theory is developed and the operation is analyzed for a superconducting nonisothermal bolometer in the regime of absolute thermal-radiation reception.

The main problem in producing an absolute thermal-radiation receiver (ATRR) is assurance of the equivalence of the electrical substitution power and the radiant thermal flux power absorbed by the ATRR sensor. One of the promising areas in the solution of this problem is the production of an ATRR based on a superconducting nonisothermal bolometer (SNB), first proposed by Franzen [1]. However, the theory worked out in [1] is developed for the two-phase state of the SNB, i.e., without taking account of the transient zone from the normal to the superconducting state, for the case when the incident thermal flux is distributed uniformly over the whole surface of the ANB sensor. This makes direct utilization of the SNB of known structures [2-4] difficult for the production of an ATRR because of the different nature of the thermal energy absorption and liberation by the bolometer sensor. In this paper a three-phase (taking account of the transient zone) theory is developed for the SNB, and computations are performed for the case when the incident thermal flux is distributed

All-Union Scientific-Research Institute of Physicotechnical and Radio Engineering Measurements, Moscow.

Translated from Inzhenerno-Fizicheskii Zhurnal, Vol. 47, No. 3, pp. 432-438, September, 1984. Original article submitted May 13, 1983.

0022-0841/84/4703-1065$08.50